DALTON

Nickel(II) N_2X_2 Schiff-base complexes incorporating pyrazole (X = NH, O or S): syntheses and characterization †

Bibhutosh Adhikhari,[a] Oren P. Anderson,*[,b] Agnete la Cour,*[,a,b] Rita Hazell,[c] Susie M. Miller,[b] Carl E. Olsen[d] and Hans Toftlund[a]

[a] *Department of Chemistry, Odense University, DK-5230 Odense M, Denmark*
[b] *Department of Chemistry, Colorado State University, Fort Collins, Colorado 80523, USA*
[c] *Department of Chemistry, Aarhus University, DK-8000 Århus C, Denmark*
[d] *Department of Chemistry, The Royal Veterinary and Agricultural University, DK-1871 Frederiksberg C, Denmark*

A series of four-co-ordinate nickel(II) N_2X_2 complexes (X = NH, O or S) with tetradentate Schiff-base ligands incorporating pyrazole has been prepared in order to compare the influence on the nickel(II) centre of the donor atoms in $N_2(NH)_2$ and N_2S_2 complexes *versus* N_2O_2 complexes. In each case, two identical parts of the ligand are linked by a two- or three-carbon aliphatic chain ($n = 2$ or 3). Crystal structures have been determined for a $n = 3$ $N_2(NH)_2$ complex, for two $n = 3$ N_2S_2 complexes and for a $n = 2$ N_2O_2 complex. All of the complexes have been investigated in solution by spectroscopic methods (UV/VIS/NIR, ^{1}H NMR). The $n = 2$ and 3 $N_2(NH)_2$ complexes and the $n = 2$ N_2S_2 complexes are fully diamagnetic. An extension of the chain linking the two halves of the ligand from two to three carbon atoms induces a spin-equilibrium process ($S = 0 \rightleftharpoons S = 1$) for the resulting N_2S_2 complex ($\Delta G = 19$–26 kJ mol^{-1} at 50 °C). Ligand-field parameters have been derived from the electronic spectra and the electrochemical properties of the N_2S_2 complexes have been investigated by cyclic voltammetry. From these results it is clear that low-spin character is emphasized in $N_2(NH)_2$ and N_2S_2 complexes of nickel(II) when compared with the corresponding N_2O_2 complexes.

It is well documented that most bis(bidentate ligand)nickel(II) N_2X_2 Schiff-base complexes incorporating pyrazole[1] exhibit pseudo-tetrahedral co-ordination (X = NH,[1a,b] O[1c,e] or S[1b,f,g]). In contrast, bis(bidentate ligand)nickel(II) N_2X_2 Schiff-base complexes based on salicylaldehydes, hydroxynaphthaldehydes or β-diketones generally exhibit planar co-ordination spheres and low-spin ($S = 0$) magnetic behavior[2] unless forced into a pseudo-tetrahedral configuration with high-spin ($S = 1$) or spin-equilibrium ($S = 0 \rightleftharpoons S = 1$) magnetic behavior by bulky substituents on the nitrogen donor atoms.[2b,3a–c]

Bis(bidentate ligand)nickel(II) N_2S_2 Schiff-base complexes, including the complexes that contain pyrazole, tend to be stabilized more in the low-spin state[1b,3a,d,e,4a] than the N_2O_2[1e,3a] and $N_2(NH)_2$[1b,2b,3b] analogues. This may be ascribed to the weak S···S bonding normally observed[4a,b] in the thiolate complexes, which results in the formation of a ligand more like a tetradentate ligand in bis(bidentate ligand) complexes and a more planar co-ordination geometry. The tendency of sulfur atoms to bond weakly to nearby sulfur atoms is also seen in metal-free systems,[4c–e] and in a complex the metal may bring about the proximity of the sulfur atoms necessary for the development of such a weak S···S bond. The S···S bonding forces the bis(bidentate ligand) N_2S_2 complexes to be *cis*[1f,g,4a,b] (the angle between the N–M–S and S–M–N planes, θ <90°). Bis(bidentate ligand) N_2O_2 and $N_2(NH)_2$ complexes seem to prefer the *trans* configuration[1b,2c,5] (θ > 90°) due to the steric requirements of substituents on the imine nitrogen donor atoms.

Comparative studies of the influence of the donor atom X on the spin state of Ni^{II} in tetradentate ligand N_2X_2 Schiff-base complexes have been almost unavailable since a tetradentate ligand tends to stabilize the planar low-spin form irrespective of X. Tetradentate ligand nickel(II) N_2X_2 complexes bridged by unsubstituted aliphatic carbon chains (X = O, $n = 2$–12;[6a–c] X = NH, $n = 2$–10[6d–f]) and incorporating aromatic carbon rings are all diamagnetic. Some results are available for tetradentate ligand nickel(II) N_2X_2 complexes based on thiosalicylaldehydes, thioacetylacetone and other thio-β-diketones, and diamines ($n = 2$–4).[3e,7,8a] The influence of sulfur seems to be similar to that established in the bis(bidentate ligand) complexes. The tetradentate ligand N_2O_2 salicylaldimine complex in which the linking unit is 2,5-dimethylhexane ($n = 4$) is fully paramagnetic, whereas the corresponding N_2S_2 complex is diamagnetic.[8a] Furthermore, tetradentate ligand N_2O_2 salicylaldimine complexes in which the linking unit is biphenyl[8b,c] exhibit spin equilibria, while an N_2S_2 analogue is diamagnetic.[8d]

In contrast to these systems that incorporate aromatic carbon rings the biphenyl-bridged nickel(II) N_2S_2 complexes incorporating pyrazole rings exhibit spin equilibria.[8d] Introduction of aromatic heterocycles as a component of Schiff-base chemistry[1g] has improved the possibilities of studying the influence of ligand modifications on the properties of metal complexes. For example, some of us have reported the properties of a series of tetradentate ligand nickel(II) N_2O_2 ketoimine and aldimine Schiff-base complexes incorporating pyrazole in which related halves of the ligands were linked by aliphatic carbon chains ($n = 2$ or 3).[9a] In another study[9b] one of us investigated a related series of N_2S_2 ketoimine complexes. In the present paper we report the preparation and properties of tetradentate ligand nickel(II) $N_2(NH)_2$, N_2S_2, and N_2O_2 complexes with aldimine Schiff-base ligands based on pyrazole ($n = 2$ or 3; see structure **A**). We do so in order to allow comparisons with the N_2O_2 aldimine[9a] and N_2S_2 ketoimine[9b] analogues, and with the corresponding N_2X_2 Schiff-base complexes ($n = 2$ or 3) incorporating unsaturated carbon rings, β-thioketoamines or β-iminoketoamines.

Results and Discussion

Syntheses and identification

Yields and some analytical data are given in Table 1 (NMR data

† *Supplementary data available* (No. SUP 57293, 8 pp.): NMR data, thermodynamic parameters, cyclovoltammetric data. See *J. Chem. Soc.*, *Dalton Trans.*, 1997, Issue 1.

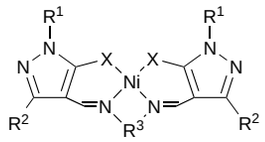

A

	n	X	R^1	R^2	R^3
1[a]	3	NH	Ph	Ph	-$(CH_2)_3$-
2	3	NH	Ph	Ph	-$CHMeCH_2CHMe$-
3[a]	2	NH	Ph	Me	-$(CH_2)_2$-
4[a]	3	NH	Ph	Me	-$(CH_2)_3$-
5	3	NH	Ph	Me	-$CHMeCH_2CHMe$-
6	3	NH	Me	Ph	-$(CH_2)_3$-
7	3	S	Ph	Ph	-$(CH_2)_3$-
8	3	S	Ph	Ph	-$CHMeCH_2CHMe$-
9	2	S	Me	Me	-$(CH_2)_2$-
10	3	S	Me	Me	-$(CH_2)_3$-
11	3	S	Me	Me	-$CHMeCH_2CHMe$-
12	2	S	Ph	Me	-$(CH_2)_2$-
13	3	S	Ph	Me	-$CHMeCH_2CHMe$-
14	3	S	Ph	Me	-$(CH_2)_3$-
15	3	S	Ph	Me	-$CHMeCH_2CHMe$-
16	2	S	Me	Ph	-$(CH_2)_2$-
17	3	S	Me	Ph	-$(CH_2)_3$-
18	3	S	Me	Ph	-$CHMeCH_2CHMe$-
19[b]	2	O	Ph	Me	-$CHMeCH_2$-

[a] First presented in ref. 10. [b] First presented in ref. 9(*a*).

are available as SUP 57293).‡ Crystals of the complexes tend to incorporate the solvent used for recrystallization, as has been observed for other $M^{II}N_2X_2$ Schiff-base complexes containing 1,3-disubstituted pyrazolyl rings ($n = 3$).[9–11,12a] Even after drying the complexes under vacuum, the results of elemental analyses can reflect small amounts of occluded solvent (see Experimental section and Table 1). Impurities were not observed in the proton NMR spectra of the complexes. Moreover, the ($n = 3$) $N_2(NH)_2$ complexes reported herein take up small amounts of water (according to microanalysis) as also seen in similar $n = 4$ $N_2(NH)_2$ complexes.[1b]

For the complexes bridged by dimethyl-substituted chains, the racemic mixture of the least-soluble diastereomer (Δ*SS*/Λ*RR*, where Δ and Λ refer to the absolute configuration of the co-ordination sphere, *R* and *S* to the configurations about the chiral centers in the dimethyl-substituted aliphatic chain) could in general be separated from other diastereomers by fractional crystallization. For example, a crystal from the first precipitate of complex **5** contained the Δ*SS* and Λ*RR* forms as established by X-ray diffraction (see below). These forms have C_2 symmetry, and the ^{1}H NMR spectra of the solutions obtained by redissolving the first precipitates of complexes **2**, **5**, **11**, **13**, **15** and **18** are simple, with only one resonance observed for each kind of proton. Subsequent precipitates contain mixtures of diastereomers in every case. Complex **8** was isolated only as a mixture of diastereomers.

Proton NMR spectra in $(CD_3)_2SO$ and electronic spectra in Me_2SO (dmso), dimethylformamide (dmf)[10] and MeCN suggest that the $N_2(NH)_2$ complexes do not increase their co-ordination number in potentially co-ordinating solvents, in contrast with the corresponding N_2O_2 complexes.[9a] The electronic spectrum of the $n = 3$ N_2S_2 complex **10** in dmso shows two weak transitions at ≈1500 nm that increase with time, which suggests that five- and four-co-ordinate complexes may be in equilibrium

‡ Complexes **3** and **4**, along with the corresponding $n = 4$ complex, were presented in ref. 10 as pyrazolyl 1-methyl-3-phenyl substituted; they should have been 3-methyl-1-phenyl substituted. The entropy change for the spin-equilibrium process for the $n = 4$ complex diphenyl pyrazolyl substituted in the same manner as in **1** was given in ref. 10 as 6 J K^{-1} mol; the correct value is 25 J K^{-1} mol^{-1}.

Table 1 Yields and analytical data for the complexes

Complex	Yield[a] (%)	Analyses (%)[b] C	H	N	EI mass spectrum *m*/*z*[c]
1[d]	87	62.25 (62.60)	4.45 (4.50)	16.45 (16.45)	620
2	20	67.10 (67.50)	5.35 (5.35)	16.95 (17.00)	648
3[d]	28	59.65 (59.65)	5.05 (5.00)	23.10 (23.20)	482
4	88	59.95 (59.85)	5.30 (5.30)	22.15 (22.35)	496
5	88	60.80 (61.20)	5.75 (5.80)	21.00 (21.15)	524
6[e]	85	57.60 (58.15)	5.45 (5.75)	21.45 (21.00)	496
7[f]	79 (59)	63.20 (63.20)	4.30 (4.25)	12.50 (12.60)	654
8[f]	83 (28)	65.00 (64.40)	4.90 (4.70)	11.90 (12.15)	682
9[d]	89 (49)	42.50 (42.75)	4.60 (4.60)	21.20 (21.40)	392
10	90 (37)	44.35 (44.25)	5.10 (4.95)	20.35 (20.65)	406
11	51 (46)	45.65 (45.50)	5.55 (5.75)	18.60 (18.75)	434
12[d]	88 (55)	55.75 (55.70)	4.30 (4.30)	16.35 (16.25)	516
13	55 (22)	56.75 (57.25)	4.85 (4.80)	14.95 (15.40)	544
14[d]	89 (53)	49.85 (49.80)	4.05 (4.00)	13.40 (13.55)	530
15	85 (50)	57.85 (57.95)	5.05 (5.05)	14.85 (15.00)	558
16[f]	77 (6)	54.55 (54.10)	4.35 (4.20)	15.35 (15.60)	516
17	90 (59)	56.45 (56.50)	4.65 (4.55)	15.70 (15.80)	530
18	54 (23)	58.10 (57.95)	5.10 (5.05)	14.85 (15.00)	558

Data for complex **19** were presented in ref. 9(*a*). [a] From ligand. Yields of pro-ligands in parentheses. [b] Calculated values in parentheses. [c] Crystal solvent, $CHCl_3$, found in complexes **1** (0.5), **7** (0.15) and **14** (0.75); CH_2Cl_2, in **6** (0.1), **8** (0.1) and **16** (0.25); or water, in **2** (0.5), **4** (0.25), **5** (0.25) and **6** (1.0), is not included in the molecular ion, M^+. [d] Recrystallized from EtOH–$CHCl_3$. [e] Recrystallized from MeOH–CH_2Cl_2. [f] Recrystallized from EtOH–CH_2Cl_2.

(also seen in the electronic spectra of similar $n = 4$ N_2S_2 complexes[1b,11]). Crystals of **10** grown from a dmso solution contain only four-co-ordinate complexes (see below) but this may only indicate that the four-co-ordinate form crystallizes more readily. The low Lewis acidity of four-co-ordinate $N_2(NH)_2$ and N_2S_2 Schiff-base complexes of Ni^{II} compared with similar N_2O_2 complexes is also observed for other families of N_2X_2 complexes with conjugated chelate rings.[3e,6d–f]

Structures of complexes 5, 10, 14 and 19

Selected bond distances and angles are listed in Table 2. The molecular structure and the asymmetric unit of complex **5** are shown in Fig. 1(*a*) and 1(*b*). The molecular structure of **10** is shown in Fig. 2, the asymmetric unit of **14** in Fig. 3, and the molecular structure and a packing diagram of **19** are seen in Fig. 4(*a*) and 4(*b*).

In complexes **5** and **14** the asymmetric unit contains two nickel(II) complexes, the Δ and Λ forms respectively. In the asymmetric unit of the centrosymmetric structure of **5** the Δ form of the complex is found to have the *S* configuration, the Λ form to have the *R* configuration at both chiral carbon atoms [C(23) and C(25)]. Crystals of both complexes diffract poorly. The molecules are bulky and difficult to pack economically, and there are no strong intermolecular forces. The distance between the nickel atoms of the asymmetric unit in complex **14** is

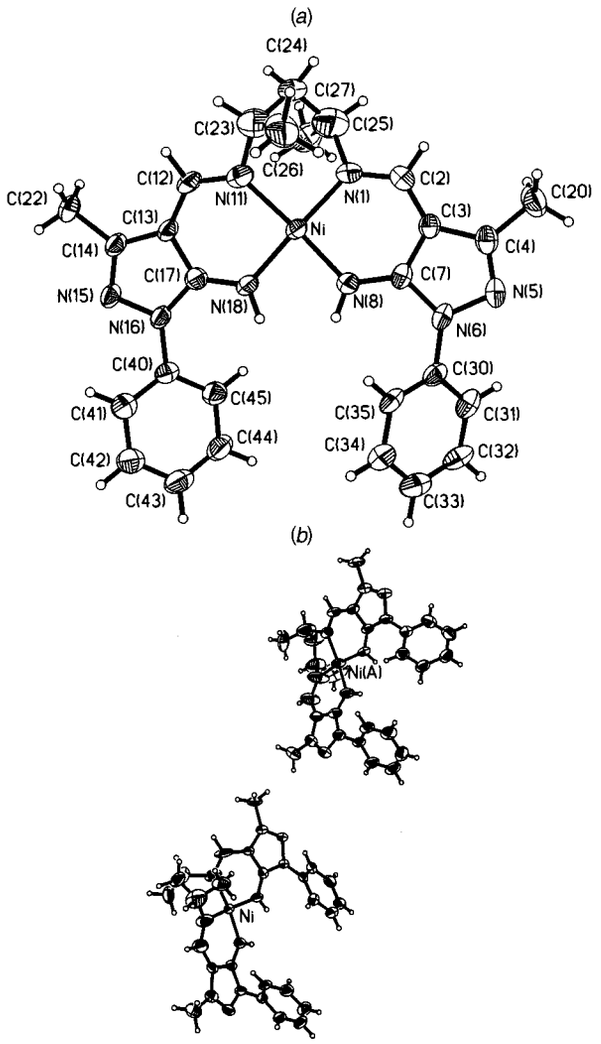

Fig. 1 Molecular structure (*a*) and asymmetric unit (*b*) for complex **5** with 50% probability thermal ellipsoids for non-hydrogen atoms

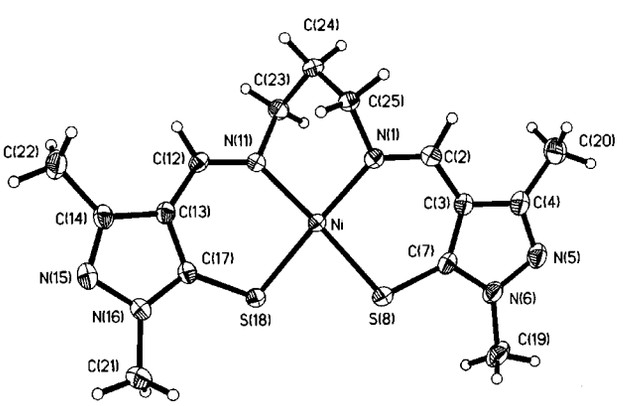

Fig. 2 Molecular structure of complex **10** with 50% probability thermal ellipsoids for non-hydrogen atoms

4.829(6) Å. Large atomic displacement parameters for C(23A)–C(27A) in complex **5** are associated with the observed disorder of the atoms connecting the two halves of the ligand; this disorder proved to be intractable to model.

The structures of complexes **5**, **10** and **14** all show a tetrahedral twist from a planar co-ordination geometry. The angles θ between the N–Ni–X planes are 17.8(5) and 15.7(6)° for the two independent complexes in the asymmetric unit of **5**, 6.9(1)° for **10** and 10.2(6) and 7.2(6)° for the two independent complexes in the asymmetric unit of **14** (see Table 2). The co-ordination geometry is close to that previously established[9a] for an $n = 3$ nickel(II) N_2O_2 phenyl ketoimine complex ($\theta = 12.7°$)[9a] with phenyl substituents on pyrazolyl groups in the same pattern as

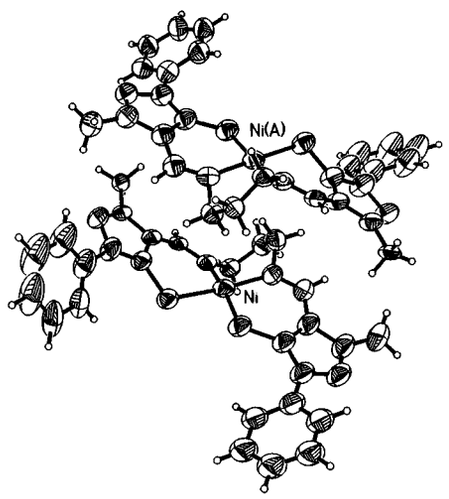

Fig. 3 Asymmetric unit for complex **14** with 50% probability thermal ellipsoids for non-hydrogen atoms. The numbering is as for complex **5** [Fig. 1(*a*)] except that the methyl substituents of the chain [C(26) and C(27)] are omitted

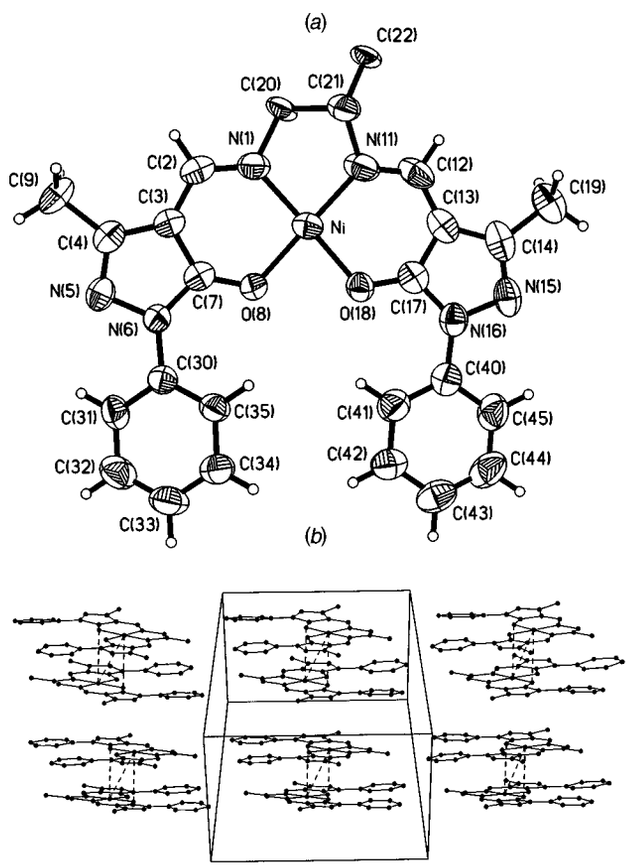

Fig. 4 (*a*) Molecular structure of complex **19** with 50% probability thermal ellipsoids for non-hydrogen atoms; one component of the disordered chain has been omitted for simplicity. (*b*) Packing diagram for **19**; the intermolecular distances Ni · · · O(8′) and Ni · · · Ni′ are 3.372(3) and 3.627(1) Å, respectively

in **1** and **7**. In contrast, the $n = 3$ nickel(II) N_2X_2 Schiff-base complexes incorporating aromatic carbon rings (benzene, naphthalene) tend to be more planar,[7b,13a,b,d] and the distortions from planarity tend to be folds rather than tetrahedral twists.[13a,b,d] The structure of **19** reveals a planar co-ordination geometry (see Table 2). The packing diagram for **19** [Fig. 4(*b*)] shows that this complex tends to form dimers in the solid state, as seen for many other N_2O_2 Schiff-base complexes of Ni^{II} and Cu^{II}.[13a–c] The Ni–L bond lengths in the four complexes are similar to those of other nickel(II) N_2X_2 Schiff-base complexes that are low spin in the solid state (X = NH,[10,13d] O[9a,13a–c]

Table 2 Selected interatomic distances (Å) and angles (°) for complexes **5**, **10**, **14** and **19** *

	5	**5A**	**10**	**14**	**14A**	**19**
Ni–N(1)	1.903(6)	1.903(8)	1.928(2)	1.97(3)	1.88(3)	1.865(4)
Ni–N(11)	1.890(7)	1.906(6)	1.942(2)	1.91(3)	1.89(3)	1.868(4)
Ni–X(8)	1.864(5)	1.877(6)	2.2057(7)	2.21(1)	2.18(1)	1.887(3)
Ni–X(18)	1.872(5)	1.859(6)	2.1926(7)	2.21(1)	2.24(1)	1.874(3)
N(1)–C(2)	1.32(1)	1.32(1)	1.297(3)	1.31(3)	1.26(3)	1.298(6)
C(2)–C(3)	1.37(1)	1.37(1)	1.422(4)	1.39(4)	1.41(4)	1.386(6)
C(3)–C(7)	1.400(9)	1.38(1)	1.389(4)	1.38(4)	1.42(4)	1.400(6)
C(7)–X(8)	1.324(8)	1.324(9)	1.725(3)	1.77(3)	1.65(3)	1.274(5)
N(11)–C(12)	1.32(1)	1.32(1)	1.298(3)	1.29(3)	1.29(3)	1.298(6)
C(12)–C(13)	1.39(1)	1.40(1)	1.418(4)	1.44(4)	1.37(4)	1.377(7)
C(13)–C(17)	1.400(9)	1.410(9)	1.398(4)	1.42(5)	1.44(4)	1.399(6)
C(17)–X(18)	1.329(8)	1.329(8)	1.725(3)	1.71(3)	1.65(3)	1.278(5)
X · · · X	2.550(7)	2.521(8)	2.851(1)	2.88(1)	2.88(1)	2.528(6)
N(1) · · · N(11)	2.674(9)	2.735(9)	2.702(3)	2.70(3)	2.70(4)	2.487(6)
N(1)–Ni–N(11)	90.0(3)	92.0(3)	88.55(9)	88(1)	92(1)	85.2(2)
N(1)–Ni–X(8)	93.8(9)	92.0(3)	96.16(6)	95.0(8)	94.7(8)	95.8(2)
N(1)–Ni–X(18)	168.8(3)	167.0(4)	173.94(7)	171.8(7)	173.4(8)	178.4(2)
N(11)–Ni–X(8)	164.7(4)	168.8(3)	173.26(7)	171.5(8)	171.9(8)	179.0(2)
N(11)–Ni–X(18)	93.1(3)	93.5(3)	94.91(6)	96.5(9)	93.0(8)	96.2(2)
X(8)–Ni–X(18)	86.1(2)	84.9(3)	80.83(3)	81.4(4)	81.3(4)	82.8(1)
Ni–N(1)–C(2)	126.2(5)	125.6(7)	129.8(2)	129(2)	135(3)	127.9(3)
N(1)–C(2)–C(3)	125.7(7)	126.1(8)	124.8(2)	124(3)	123(3)	122.5(4)
C(2)–C(3)–C(7)	122.1(6)	121.1(7)	125.5(2)	127(3)	124(3)	122.4(4)
C(3)–C(7)–X(8)	126.3(6)	126.4(6)	128.9(2)	126(3)	129(3)	130.4(4)
Ni–X(8)–C(7)	125.9(5)	125.4(5)	104.19(9)	105(1)	107(1)	120.6(7)
Ni–N(11)–C(12)	127.0(6)	126.1(6)	129.7(2)	132(3)	133(2)	126.8(4)
N(11)–C(12)–C(13)	124.6(7)	125.3(7)	124.4(2)	123(4)	124(3)	123.4(4)
C(12)–C(13)–C(17)	121.6(6)	122.3(7)	124.4(2)	129(3)	122(3)	122.5(5)
C(13)–C(17)–X(18)	126.3(6)	124.7(7)	129.1(2)	125(3)	132(2)	130.4(5)
Ni–X(18)–C(17)	124.9(4)	127.0(5)	103.19(9)	107(1)	101(1)	121.0(3)
Angles θ (°) between planes						
N(1)–Ni–X(8) / X(18)–Ni–N(11)	17.8(5)	15.7(6)	6.9(1)	10.2(6)	7.2(6)	0.7(3)
Selected torsion angles (°)						
N(5)–N(6)–C(30)–C(31)	151.3(6)	−149.3(7)	—	41(2)	43(2)	18.7(6)
N(15)–N(16)–C(40)–C(41)	−30.0(8)	140.7(7)	—	32(2)	47(2)	−178.8(4)

* Estimated standard deviations (e.s.d.s) of the least significant digits are given in parentheses. For complexes **5** and **14** parameters for both molecules of the asymmetric unit (**5/5A**, and **14/14A**) are shown. The symbol X denotes N (**5/5A**), S (**10**, **14/14A**) or O (**19**).

or S [7b–d,13e–g]). It is seen from torsion angles for **5** and **14** (Table 2) that the pyrazole rings are not coplanar with the phenyl substituents. In **19** the phenyl rings are almost coplanar with the pyrazole rings as also seen in a similar $n = 3$ N_2O_2 complex.[9a]

Complexes **10** and **19** were both crystallized from the potential donor solvent dmso. However, in spite of spectroscopic indications that the four-co-ordinate complexes are in equilibrium with five- [**10**, this work; see also refs. 1(*b*) and 11 for similar cases] or six-co-ordinate complexes [**19**, ref. 9(*a*)] in solution, the four-co-ordinate complex crystallizes more readily.

Magnetic properties

All complexes are low spin in the solid state as indicated by the magnetic moments (μ = 0.52–1.14 μ_B at 23 °C; $\mu_B \approx 9.27 \times 10^{-24}$ J T^{-1}). The weak paramagnetism observed is mainly due to temperature-independent paramagnetism.[8d]

Temperature-dependent (25–50 °C) ^{1}H NMR spectra for representative complexes in $CDCl_3$ reveal that the $n = 3$ N_2S_2 complexes (see Table 3) are in spin equilibrium ($S = 0 \rightleftharpoons S = 1$) in solution, as were the related N_2O_2 complexes.[9a] The chemical shifts of protons such as the chain proton, H_a, closest to the nitrogen donor atom and of the imine proton, H_c, are temperature dependent; the chemical shift becomes more positive due to an increase in the paramagnetic isotropic Fermi contact shift with temperature. For the $n = 2$ N_2S_2 complexes and for all $N_2(NH)_2$ complexes the shifts are practically temperature independent or are at *less* positive δ values with increasing temperature (protons H_c in particular). The coupling constant A_c is negative, corresponding to *more* positive δ_c values with temperature, for the $n = 3$ N_2S_2 complexes and for other pyrazolyl-containing N_2X_2 complexes [1b,10,13f,g] ($n = 4$, X = NH or S). The temperature dependence in these cases is therefore ascribed to conformational changes and not to a spin-equilibrium process. Complex **19** has been shown previously [9a] to be fully diamagnetic in non-donor solvents. The temperature-dependent ^{1}H NMR spectra show that if $n = 3$ the nickel(II) $N_2(NH)_2$ complexes are more stabilized in the low-spin state than are both the nickel(II) N_2O_2 and N_2S_2 complexes.

The chemical shifts of protons H_a and H_c were used to evalu-

Table 3 Thermodynamic parameters for the spin-equilibrium process *

Complex	Δ*H* /kJ mol^{-1}	Δ*S* /J K^{-1} mol^{-1}	Δ*G* (50 °C) /kJ mol^{-1}
7	30.0 ± 7.4	13.7 ± 17.9	25.6 ± 1.6
10	22.6 ± 0.0	9.36 ± 0.86	19.6 ± 0.3
11	22.3	16.9	16.8
14	24.7 ± 0.8	4.92 ± 2.27	23.1 ± 0.1
15	21.8	7.49	19.4
17	23.2 ± 0.1	2.43 ± 2.97	22.4 ± 1.1
18	22.0	8.79	19.2

* Measured in $CDCl_3$; e.s.d.s are given only for complexes bridged by unsubstituted propylene chains (see the text). Correlation coefficients of the van't Hoff plots were >0.99.

ate equilibrium constants for the spin-equilibrium process for the complexes listed in Table 3 by a method described previously[9a] (see Experimental section for details); ΔH and ΔS were derived from the van't Hoff plots (Table 3). For the complexes in which the ligands contained dimethyl-substituted chains, a coupling constant A_a, for a paramagnetic reference was not available for H_a, and only the chemical shifts of H_c were used to assess the thermodynamic parameters for these complexes (**11**, **15** and **18**). The use of chemical shifts for H_a for the remaining complexes yields results consistent with those obtained by the use of chemical shifts for H_c. The parameters listed in Table 3 are for each complex the average values of those obtained from the two van't Hoff plots based on chemical shifts for H_a and H_c, respectively. The uncertainties of the parameters are large, however, for the least paramagnetic spin-equilibrium system, the diphenylpyrazolyl-containing complex **7**.

In general, the high-spin state is less favoured for the N_2S_2 complexes listed in Table 3 than in the $n = 3$ N_2O_2 ketoimine complexes incorporating pyrazole,[9a] mainly due to more positive enthalpy changes (see also Fig. 5 below). As was the case for the N_2O_2 complexes,[9a] the entropy changes are small and probably result from the few degrees of rotational freedom gained for the ligand substituents in the slightly less crowded pseudo-tetrahedral configuration. The more positive ΔS values for the complexes bridged by methyl-substituted chains (**11**, **15** and **18**) than for the unsubstituted analogues (**10**, **14** and **17**) are expected for steric reasons.

Electronic spectra

The ligand-field spectra (see Table 4) are similar to those of the N_2O_2 analogues,[9a] and the assignments for those analogues[9a] have been used in the present work. (D_{4h} symmetry is assumed with the donor atoms on the Cartesian x and y axes.) Ligand-field parameters were derived using the method of ref. 9(*a*). Since the $^1B_{1g}$ transition is seen only as a shoulder, the uncertainties of the ligand-field parameters derived in this work are larger than for the N_2O_2 complexes previously studied.[9a]

In our earlier work,[9a] the spectra of the $n = 3$ N_2O_2 pro-ligands were only slightly influenced by complexation with Ni^{II}. In contrast, the spectra of the $N_2(NH)_2$ and the N_2S_2 pro-ligands in the present work were more substantially changed (see Table 5) on complexation with Ni^{II}. Therefore, more covalency in the M–L bonds and stronger nephelauxetic effects are expected for the $N_2(NH)_2$ and N_2S_2 complexes. In fact, such effects have been observed[1b,d,8d] in related systems and are in accord with expected trends.[15a] Values of B in related complexes have been found to be influenced by substitution on the aliphatic chain.[1b] Similar influences are assumed to apply to the complexes investigated in this work.

For $N_2(NH)_2$ systems (**1**–**6**) the effect of a chain extension from two to three carbon atoms is a significant decrease of the ligand field. This is normal for $N_2(NH)_2$[6d–f,14a] and N_2O_2[9a] Schiff-base complexes. In nickel(II) $N_2(NH)_2$ complexes incorporating pyrazole an increase in chain length to four carbon atoms induces the spin-equilibrium process at temperatures significantly below room temperature.[1b,10]

Based on the e_σ and $e_{\pi\|}$ values,§ the $N_2(NH)_2$ ligands are both stronger σ and π donors than are the N_2O_2 analogues;[9a] based on the Δ_1 and Δ_1/B values, the ligand fields and ligand-field strengths are larger in the $N_2(NH)_2$ complexes. These tendencies are expected[6d] and are in accord with the temperature-dependent ^1H NMR results above and in ref. 9(*a*).

The N_2S_2 ligands are both weaker σ and π donors than are the N_2O_2 and $N_2(NH)_2$ analogues. The effects of an increase in chain length are small and comparable with the substitution effects. Similar weak effects of a chain extension have been observed for other N_2S_2 Schiff-base complexes.[7b,14b,c] However, as seen for analogous nickel(II) $N_2(NH)_2$ complexes,[1b,10] the high-spin population of the nickel(II) N_2S_2 complexes increases dramatically on extension of the chain from three to four carbon atoms.[1b,8d,13f,g]

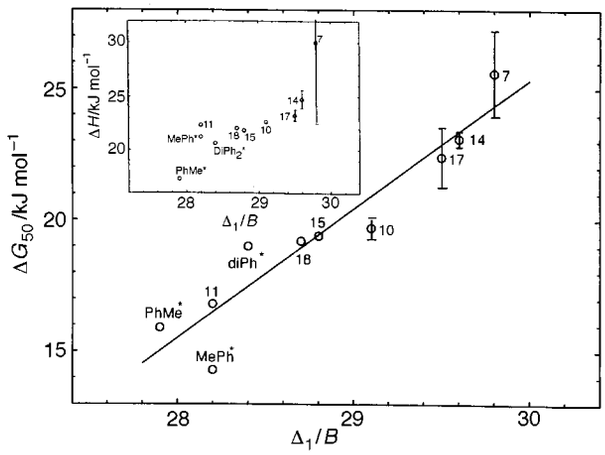

Fig. 5 Plots of ΔG(50 °C) and ΔH (inset) against Δ_1/B. Complexes labelled with an asterisk are the nickel(II) N_2O_2 ketoimine complexes of ref. 9(*a*) analogous to **7** (Ph_2), **14** (PhMe) and **17** (MePh) where the substituents are those of pyrazolyl

The quotient Δ_1/B establishes the following trend in ligand-field strength: X = O < S ≈ N. This is the same order established by the thermodynamic measurements of N_2O_2 and N_2S_2 complexes (see Fig. 5 and discussion of NMR results above). From these results, it should be clear that low-spin character is emphasized in $N_2(NH)_2$ and N_2S_2 complexes of nickel(II) when compared with the corresponding N_2O_2 complexes.

Ligand-field parameters derived from reported spectra for other $n = 2$ or 3 N_2X_2 Schiff-base complexes are listed in Table 4 for comparison. The $N_2(NH)_2$ and N_2S_2 complexes incorporating benzene, [Ni(asaltn)],[6f] [Ni(tsalen)],[7b] [Ni(tsaltn)],[7b] or thioacetylacetonimine, [Ni(tacacen)],[7d] are significantly more stabilized in the low-spin state than the pyrazole-based complexes in agreement with the results obtained for the N_2O_2 complexes.[9a] The parameters for the N_2S_2 ketoimine ($\mathbf{12}_{keto}$ and $\mathbf{14}_{keto}$) complexes[9b] analogous to **12** and **14** and for the $n = 2$ or 3 N_2S_2 aldimine complexes incorporating cyclopentene [Ni(pent-en), Ni(pent-tn)][14b] are comparable with those of N_2S_2 aldimine complexes investigated in this work. Parameters for the low-spin form of some $n = 4$ or 5 spin-equilibrium systems, [Ni(bi-Ph)],[8d] [Ni(pent-bn)],[14b] [Ni(pent-pn)],[14c] are also listed. With $B \approx 850$ cm^{-1} for the paramagnetic tetrahedral form the change of spin-pairing energy[16] in going from $S = 0$ to 1 is about $-12\,000$ cm^{-1}, and a tetrahedral field Δ_{Td} of ≈5000 cm^{-1} is expected for the pseudo-tetrahedral form in the spin-equilibrium mixture. This is close to the Δ_{Td} of ≈4500 cm^{-1} found for $n = 4$ pyrazole-based N_2S_2 spin-equilibrium systems.[1b,8d]

Charge-transfer (CT) and intraligand (IL) transitions and spectral data for the nickel(II) complexes and for the protonated pro-ligands are given in Table 5. The intensities and the resemblance with the protonated pro-ligands suggest that the transitions below 320 nm are $\pi \rightarrow \pi^*$ IL transitions. For the N_2S_2 complexes the transition between 335 and 350 nm is also ascribed to a $\pi \rightarrow \pi^*$ IL transition, as the first transition ($\varepsilon \approx 10\,000$ dm^3 mol^{-1} cm^{-1}) is found at that position for zinc(II) complexes with similar ligands.[12a,13g] The remaining bands are assigned to CT transitions.

Electrochemistry of the N_2S_2 complexes

Previous work has shown that electrochemical processes for the

§ Only the in-plane π interaction can be evaluated from the spectra, as the ^1E_g transition was not observed. For the N_2O_2 complexes, the in- and out-of-plane π interactions are similar.[15b] For the $N_2(NH)_2$ complexes, the nature of the out-of-plane π interaction is uncertain.[15b]

Table 4 Ligand-field transitions and parameters[a]

Complex	Transition			e_σ	$e_{\pi\parallel}$	Δ_1[b]	e_σ/e_π	Δ_1/B
	$^3\Gamma$	$^1A_{2g}$	$^1B_{1g}$					
X = NH								
1[c] ($n = 3$)		16 000 (125)	21 275 (sh) (295)	7965	1345	18 515	5.9	29.6
2[c] ($n = 3$)		15 950 (123)	21 055 (sh) (280)	7895	1310	18 445	6.0	29.5
3[c] ($n = 2$)		16 780 (147)		8265	1375	19 295	6.0[d]	30.9
4[c] ($n = 3$)		15 675 (105)	21 000 (sh) (180)	7880	1365	18 180	5.8	29.1
5[c] ($n = 3$)		15 550 (104)	20 835 (sh) (225)	7830	1360	18 050	5.8	28.9
6[c] ($n = 3$)		15 725 (124)	20 835 (sh) (175)	7830	1315	18 230	6.0	29.2
[Ni(asaltn)][c,e] ($n = 3$)		16 350[6f]		8080	1345	18 860	6.0[d]	30.2
X = S								
7[f] ($n = 3$)		15 455 (108)	20 000 (sh) (160)	7515	1170	17 865	6.4	29.8
8[c] ($n = 3$)		15 625 (114)	19 610 (sh) (170)	7455	1060	18 125	7.0	29.0
9[f] ($n = 2$)		15 290 (108)	20 000 (sh) (130)	7515	1215	17 685	6.2	29.5
10[f] ($n = 3$)	12 820 (sh) (25)	15 085 (97)	19 085 (sh) (120)	7240	1055	17 500	6.9	29.1
11[c] ($n = 3$)	12 500 (sh) (30)	15 315 (107)	18 690 (sh) (145)	7180	930	17 640	7.7	28.2
12[f] ($n = 2$)		15 455 (73)	20 000 (sh) (105)	7515	1170	17 865	6.4	29.8
13[f] ($n = 3$)		15 505 (101)	20 000 (sh) (140)	7515	1160	17 905	6.5	29.8
14[f] ($n = 3$)	13 070 (sh) (35)	15 360 (100)	19 400 (sh) (170)	7335	1060	17 765	6.9	29.6
15[c] ($n = 3$)	12 500 (sh) (25)	15 500 (sh) (100)	19 050 (sh) (175)	7290	965	18 010	7.6	28.8
16[f] ($n = 2$)		15 410 (111)	20 000 (sh) (155)	7515	1185	17 805	6.3	29.7
17[f] ($n = 3$)		15 290 (143)	19 410 (sh) (140)	7335	1080	17 685	6.8	29.5
18[c] ($n = 3$)	12 660 (sh) (30)	15 430 (142)	19 050 (sh) (165)	7285	985	17 915	7.4	28.7
$\mathbf{12}_{keto}$[f,g] ($n = 2$)		15 600[9b]		7580	1185	18 000	6.4[d]	30.0
$\mathbf{14}_{keto}$[f,g] ($n = 3$)		15 410[9b]		7335	1050	17 805	7.0[d]	29.7
[Ni (biPh)][c,h] ($n = 4$)		≈14 500[8d]		6890	920	17 000	7.5[d]	27.2
[Ni (tsalen)][f,i] ($n = 2$)		16 670[7b]		8030	1255	19 070	6.4[d]	31.8
[Ni (tsaltn)][f,j] ($n = 3$)		16 530[7b]		7800	1115	18 780	7.0[d]	31.3
[Ni (tacacen)][f,k] ($n = 2$)		16 530[7d]		7970	1245	18 930	6.4[d]	31.3
[Ni (pent-en)][f,l] ($n = 2$)		15 150[14b]		7390	1155	17 550	6.4[d]	29.3
[Ni (pent-tn)][f,l] ($n = 3$)		14 950[14b]		7145	1020	17 355	7.0[d]	28.9
[Ni (pent-bn)][c,l] ($n = 4$)		14 750[14b]		6995	935	17 245	7.5[d]	27.6
[Ni (pent-pn)][c,l] ($n = 5$)		14 400[14c]		6850	915	16 890	7.5[d]	27.0

[a] Measured in $CHCl_3$ at 25 °C; energies in cm^{-1}, absorption coefficients listed in parentheses in $dm^3\ mol^{-1}\ cm^{-1}$; sh = shoulder; the ground state is $^1A_{1g}$. [b] $\Delta_1 = 3e_\sigma - 4e_\pi$. [c] $B = 625\ cm^{-1}$. [d] Estimated. [e] *o*-Aminobenzylideneimine complex.[6f,f] $B = 600\ cm^{-1}$. [g] Ketoimine complex[9b] pyrazolyl substituted in the same manner as for **12** and **14**. [h] Biphenyl-bridged complex incorporating pyrazole.[8d] [i] Ref. 7(*b*). H_2tsalen = *N*,*N*′-Bis(thiosalicylidene)ethane-1,2-diamine. [j] Ref. 7(*b*). H_2tsaltn = *N*,*N*′-Bis(thiosalicylidene)propane-1,3-diamine. [k] Ref. 7(*d*). H_2tacacen = 4,4′-Ethylenedinitrilobis(pentane-2-thione). [l] Refs. 14(*b*) and 14(*c*).

N_2S_2 Schiff-base pyrazolyl-containing ligands and zinc(II) complexes are very slow.[12a] Voltammetric data for the nickel(II) N_2S_2 complexes in acetonitrile are listed in Table 6. Results for the $n = 3$ N_2O_2 ketoimine complex analogous to **14** (NiN_2O_2)[9a] measured under the same conditions are listed for comparison. However, most N_2O_2 complexes described in ref. 9(*a*) are too insoluble in acetonitrile for electrochemical measurements. Results for the $n = 2$ or 3 N_2S_2 ketoimine complexes[9b] analogous to **12** and **14** ($\mathbf{12}_{keto}$, $\mathbf{14}_{keto}$) are also listed.

The Ni^{II}–Ni^{III} oxidation is in most cases partly obscured by a wave arising from ligand oxidation ($E_{ox} = 0.80$ to 0.92, $E_{red} = -0.39$ to -0.11, $E_{\frac{1}{2}} = 0.17$ to 0.48, $\Delta E = 0.91$ to 1.33 V). For **12** and **14** the metal oxidation is a reversible one-electron process, and in every case Ni^{II} is quasi-reversibly reduced to Ni^{I} (see Fig. 6 for complex **14**).

The pyrazole-based complexes listed in Table 6 are more easily reduced than the nickel(II) N_2S_2 complexes incorporating unsaturated carbon rings.[14b,17a] This arises from (1) weaker ligand fields and (2) stronger nephelauxetic effects for the former complexes.

Regarding the ligand-field effects, the $M^{II}N_2S_2$ complexes previously investigated[9b,14b,17b,c] showed reduction potentials inversely correlated with ligand-field strengths. For example, an extension of the chains in tetradentate ligand complexes decreases the ligand field and increases the potential for the reduction of the metal. This same trend is observed for the $n = 2$

Table 5 Charge-transfer and intraligand transitions[a]

Complex	
X = NH	
1	397 (6160), 380 (sh) (5650), 320 (sh) (21 900), 278 (56 100)
2	395 (sh) (5610), 383 (5790), 330 (sh) (16 400), 293 (48 000)
3	439 (2170), 391 (5490), 375 (sh) (4410), 310 (sh) (23 800), 290 (sh) (28 400), 265 (40 800)
4	394 (5220), 385 (sh) (5090), 310 (sh) (20 200), 268 (37 200)
5	390 (sh) (4410), 377 (4660), 325 (sh) (21 900), 287 (50 500)
6	395 (6330), 380 (sh) (5860), 320 (sh) (15 000), 279 (44 400)
HL[b]	327 (20 000), 265 (20 000)
X = S	
7	400 (sh) (2510), 350 (sh) (10 400), 297 (69 000), 259 (87 100)
8	400 (sh) (2680), 350 (sh) (9010), 299 (57 200), 260 (76 900)
9	400 (sh) (2150), 381 (3170), 340 (sh) (7170), 320 (sh) (8130), 290 (sh) (35 700), 267 (68 900)
10	380 (sh) (2420), 340 (sh) (6710), 295 (34 900), 265 (64 600)
11	380 (sh) (2380), 340 (sh) (6680), 297 (27 600), 264 (58 900)
12	392 (2530), 350 (sh) (8360), 335 (9440), 293 (44 000), 260 (46 900)
13	395 (2580), 345 (sh) (9080), 337 (9250), 291 (52 100), 256 (48 400)
14	410 (sh) (2140), 350 (sh) (8060), 310 (sh) (29 300), 288 (47 700), 258 (49 700)
15	395 (sh) (2180), 350 (sh) (7110), 310 (sh) (22 800), 291 (31 000), 285 (sh) (30 300), 255 (sh) (38 900)
16	405 (sh) (2400), 380 (sh) (3710), 345 (sh) (12 260), 331 (13 400), 286 (52 600)
17	390 (sh) (2450), 345 (sh) (10 800), 294 (55 900), 284 (56 500)
18	390 (sh) (2450), 340 (sh) (8880), 294 (31 500), 281 (31 100)
H_2L[c]	≈400 (≈10 000), ≈320 (≈20 000), ≈290 (>20 000)

[a] Measured in $CHCl_3$ at 25 °C; wavelengths in nm, absorption coefficients in parentheses in $dm^3\ mol^{-1}\ cm^{-1}$. [b] Pro-ligand (X = NH) incorporating pyrazole [from ref. 1(*a*)]. [c] Pro-ligands for complexes **7**–**18** (X = S).

Table 6 Voltammetric results for the nickel(II) N_2S_2 complexes[a]

Complex	*n*	Δ*E*/V	$E_{\frac{1}{2}}$/V
7[b]	3	0.071	−1.143(3)
8[b]	3	0.072	−1.131(3)
9[b]	2	0.083	−1.339(6)
10[c]	3	0.075	−1.178(2)
11[c]	3	0.125	−1.205(6)
12[b]	2	0.085	−1.308(11)
14[c]	3	0.065	−1.124(2)
15[c,d]	3	0.082	−1.129(2)
16[b]	2	0.091	−1.327(3)
17[c]	3	0.080	−1.158(6)
18[c]	3	0.081	−1.160(2)
$\mathbf{12}_{keto}$[e]	2	0.060	−1.24
$\mathbf{14}_{keto}$[e]	3	0.058	−1.16
NiN_2O_2[b,d,f]	3	0.14	−1.27

[a] Data for the Ni^{II}–Ni^{I} reduction are listed; e.s.d.s of the least significant digits are given in parentheses; measured in MeCN *vs*. Ag–AgCl; sweep rate 100 mV s^{-1}; voltammetric data for the $N_2(NH)_2$ complexes **1**, **3** and **4** measured in dmf are given in ref. 10. [b] Complex concentration 0.5 mmol dm^{-3}. [c] Complex concentration 1 mmol dm^{-3}. [d] The process is partly irreversible: reduction peak > reoxidation peak. [e] The N_2S_2 ketoimine complexes[9b] pyrazolyl substituted as in **12** and **14** (measured in MeCN at a mercury-film electrode). [f] Nickel(II) N_2O_2 ketoimine complex[9a] pyrazolyl substituted as in **14** measured under the same conditions as for the N_2S_2 complexes described in this work; voltammetric results for the N_2O_2 complexes in CH_2Cl_2 are given in ref. 9(*a*).

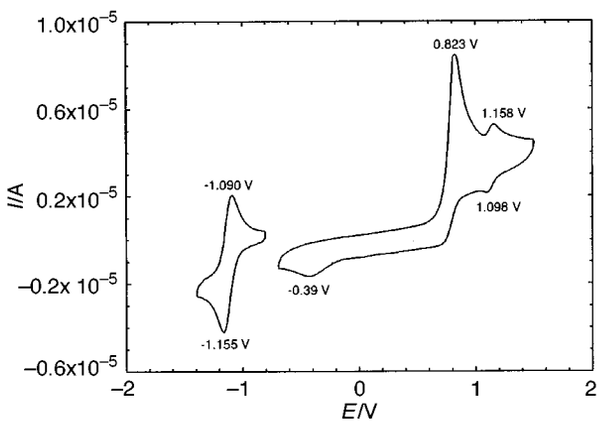

Fig. 6 Cyclic voltammogram for complex **14** in MeCN *vs*. Ag–AgCl; the sweep rate is 100 mV s^{-1}. The anodic process shown by the peaks at 0.823 and −0.39 V is assigned to ligand oxidation ($E_{\frac{1}{2}}$ = 0.22, Δ*E* = 1.21 V); the anodic process shown by the peaks at 1.158 and 1.098 V is assigned to a reversible Ni^{II}–Ni^{III} oxidation ($E_{\frac{1}{2}}$ = 1.127, Δ*E* = 0.060 V), see Table 6 for the metal-based reductions.

or 3 nickel(II) N_2S_2 complexes of the present work and of refs. 9(*b*) and 14(*b*). The inverse correlation between the reduction potential and the ligand-field strength has been ascribed to an easier access for the incoming electron to a less antibonding metal σ* ($d_{x^2-y^2}$) orbital in the less ligand-field-stabilized complex.[9b]

Stronger nephelauxetic effects lower the interelectronic repulsions on the metal ion, which then becomes more easily reducible.[15a] The electron-withdrawing effects of the nitrogen atoms of the pyrazole rings reduce the σ-electron density on the metal and lower the magnitude of *B*.[13g] In previously investigated $n = 4$ $M^{II}N_2S_2$ Schiff-base complexes (M = Ni or Cu) incorporating cyclopentene,[14b,17b] pyrazole,[13g] isoxazole,[13g] or pyridinium[17c] the half-wave potentials for the Cu^{II}–Cu^{I} reduction are −640, −407, 3 and 200 mV, respectively. The same order is found for the Ni^{II}–Ni^{I} reduction,[13g,14b] except that data for nickel(II) complexes with incorporated pyridinium are not available. This order is expected based on the electron-withdrawing effects of the incorporated rings. Ligand-field considerations alone (see Table 4) would predict similar potentials for the complexes incorporating cyclopentene and pyrazole. Additionally, comparisons of differently 1,3-disubstituted pyrazolyl-containing complexes with the same chain length (Table 6) show that the phenyl-substituted complexes [**7**, **8**, **14**, **15**, **17** and **18** ($n = 3$); **12** and **16** ($n = 2$)] in spite of stronger ligand fields (Table 4) are easier to reduce than the dimethyl-substituted complexes [**10** and **11** ($n = 3$), **9** ($n = 2$)]. This is also seen in a series of $n = 4$ nickel(II) N_2S_2 complexes incorporating pyrazole[11] and is ascribed to the inductive effects of the substituents.

Experimental

Materials

Most chemicals used were reagent grade and commercially available, used as received. Solvents used for analytical

Table 7 Crystal data and details of data collection and structure refinement for complexes **5**, **10**, **14** and **19**

	5	**10**	**14**	**19**
Formula	$C_{27}H_{30}N_8Ni$	$C_{15}H_{20}N_6NiS_2$	$C_{25}H_{24}N_6NiS_2$	$C_{25}H_{24}N_6NiO_2$
M	525.30	407.20	531.33	493.16
Crystal system	Monoclinic	Monoclinic	Monoclinic	Monoclinic
Space group	$P2_1/c$	$P2_1/c$	$P2_1$	$P2_1/c$
a/Å	23.1532(4)	13.1393(3)	10.165(9)	8.6235(2)
b/Å	10.8755(1)	9.5415(2)	22.04(1)	13.2402(3)
c/Å	22.0478(3)	14.0097(4)	11.146(8)	19.5375(2)
β/°	105.607(1)	94.185(1)	92.03(4)	93.263(1)
U/Å^3	5347.0(1)	1751.69(7)	2496(3)	2227.11(8)
Crystal size/mm	0.42 × 0.28 × 0.08	0.40 × 0.28 × 0.08	0.46 × 0.34 × 0.26	0.40 × 0.20 × 0.10
D_c/g cm^{-3}	1.30	1.54	1.41	1.47
Z	8	4	4	4
μ/cm^{-1}	7.56	13.6	9.65	9.07
Transmission factors	0.697–0.862	0.702–0.862	—	0.641–0.942
θ Limits/°	1–23	2–23	0–20	2–28
Octants collected[a]	±h, ±k, ±l	±h, ±k, ±l	±h, +k, +l	±h, ±k, ±l
Standard reflections measured	—	—	2 every 50	—
Fall-off corrected for (%)	—	—	4	—
No. of unique data	7647[b]	2513[b]	2405	5389[b]
No. data with $I/\sigma(I)>2$	6123[b]	2217[b]	1548	3012[b]
No. variables	650	218	210	335
R	0.081[c]	0.027[c]	0.087[d]	0.068[c]
wR	0.195[c]	0.068[c]	0.085[d]	0.153[c]
S	1.022	1.052	1.71	1.041
$(\Delta/\sigma)_{max}$	0.2	0.001	0.3	1.0
$\Delta\rho_{max}$, $\Delta\rho_{min}$/e Å^{-3}	1.43,[e] −0.75	0.38, −0.30	0.62, −0.45	0.56, −0.48

[a] Followed by merging in the case of complexes **5**, **10** and **19**. [b] Merged data. [c] Refinement on F^2; $R = \Sigma(||F_o| - |F_c||)/\Sigma|F_o|$, $wR = [\Sigma w(F_o^2 - F_c^2)^2/\Sigma w(F_o^2)^2]^{\frac{1}{2}}$, $w^{-1} = \sigma^2F_o^2 + (0.0546P)^2 + 30.8007P$ for **5**, $\sigma^2F_o^2 + (0.0380P)^2 + 2.0751P$ for **10** and $\sigma^2F_o^2 + (0.0722P)^2 + 2.7095P$ for **19**; $P = (F_o^2 + 2F_c^2)/3$. [d] Refinement on F; $R = \Sigma(||F_o| - |F_c||)/\Sigma|F_o|$, $wR = [\Sigma w(|F_o| - |F_c|)^2/\Sigma w|F_o|^2]^{\frac{1}{2}}$, $w^{-1} = \{[\sigma_c(F^2) + 1.03F^2]^{\frac{1}{2}} - |F|\}^2$. [e] 1.35 Å from C(24).

purposes were spectroscopic grade. Acetonitrile used for electrochemical measurements was refluxed over phosphorus pentaoxide and distilled immediately before use.

Preparations

2,3-Diaminobutane,[18] 2,4-diaminopentane,[19] the N_2S_2 Schiff bases,[12a] and the N_2S_2 complexes[13g] were prepared according to literature methods.

Nickel(II) $N_2(NH)_2$ complexes. The following general procedure was used. A suspension of the appropriate *o*-aminopyrazolecarbaldehyde (3.8 mmol) prepared according to ref. 20 was stirred in absolute ethanol (7 cm^3) at reflux temperature. The appropriate diamine (3.8 mmol) and nickel(II) acetate tetrahydrate (3.8 mmol) were added. The mixture was stirred at reflux temperature for 20 min. In most cases the dark green complex precipitated during that period. The product was filtered off and washed with 96% ethanol on the filter-paper. In the case of **5** the product-containing solution was concentrated to about half the original volume, and the complex crystallized after a few days. It was collected and used without further purification.

Physical measurements

Proton NMR spectra of pro-ligands and complexes in $CDCl_3$ and $(CD_3)_2SO$ were obtained on Bruker AC250 spectrometers equipped with VT1000 temperature controllers. The uncertainty of the temperature was less than 1 °C. Assignments were accomplished by comparisons with similar systems; $SiMe_4$ was used as internal standard.

Electrochemical data for the N_2S_2 complexes in MeCN (0.5–1 mmol dm^{-3}) were collected under N_2 by cyclic voltammetry at room temperature using microelectrodes from BAS100 (platinum working and counter electrodes, a water-based Ag–AgCl reference electrode). Ferrocene was used as an external standard [$E_{\frac{1}{2}}(Fe^{II}–Fe^{III}) = 500$ mV under the given conditions]. The sweep rate was 50–300 mV s^{-1}. The supporting electrolyte, NBu_4PF_6, and the complexes were dried in vacuum immediately before use. The electrolyte solution (0.1 mol dm^{-3}) was scanned before adding complex to check its purity.

Electronic absorption spectra were obtained in a 1 cm quartz cuvette on a thermostatted Shimadzu UV-3100 apparatus. The electron impact mass spectra were obtained on a Finnigan Mat SSQ710 or a Varian Mat 311A apparatus. Magnetic susceptibilities were measured in the solid state at 23 °C by using a Sherwood Scientific magnetic susceptibility balance. Diamagnetic corrections were made by using Pascal's constants. Elemental analyses were performed at the H. C. Ørsted Institute, University of Copenhagen. The complexes were dried 24 h in vacuum before elemental analyses.

Determination of thermodynamic parameters for the spin-equilibrium process

Equilibrium constants for the spin-equilibrium process in $CDCl_3$ were evaluated from the temperature-dependent ^{1}H NMR spectra of protons H_a and H_c over the temperature range 25–50 °C by the method described in ref. 9(*a*). The chemical shifts for the protons of a spin-equilibrium system vary almost linearly with temperature when the system is close to the diamagnetic ground state.[1b] This was the case in this work, and the diamagnetic reference points used ($\delta_{a,dia}$ and $\delta_{c,dia}$) are the chemical shifts of H_a and H_c at −10 °C found by extrapolation from the two lowest-temperature measurements. Coupling constants found for similar pyrazolyl-containing nickel(II) complexes[1b] were used: A_a, A_c, $R^1 = R^2 = Ph$ −1.432, −3.500 G; $R^1 = R^2 = Me$ −1.432, −3.643 G; $R^1 = Ph$, $R^2 = Me$ −1.480, −3.354 G; $R^1 = Me$, $R^2 = Ph$ −1.780, −4.303 G (1G = 2.8 MHz).

Crystallography

The diffraction experiments employed Mo-Kα radiation (λ = 0.710 73 Å). Crystals of complexes **10** and **19** were grown from dmso, those of **14** from ethanol. For complex **5**, crystals from the first precipitate collected after the preparation (see above) were used for the diffraction experiment. All crystals

were dark green. Data were collected for **14** at 21 °C, and for **5**, **10** and **19** at −110 °C. The routine XP in SHELXTL [21a] was used to prepare the diagrams. Details of the X-ray diffraction experiments are given in Table 7.

Room-temperature structure of complex 14. For complex **14** data were collected on a Huber four-circle diffractometer. The data were processed as previously described [21b] and were corrected for Lorentz-polarization effects. The structure was solved by direct methods (SHELXS 86 [21c]) and refined by least-squares full-matrix refinement using a modification of ORFLS.[21d,e] Given the limitations of the data set it was appropriate to use constraints during the refinements in order to limit the number of parameters: (1) all four phenyl groups were constrained to *mm*2 symmetry; (2) displacement parameters were constrained to the TLS rigid-body model as described in ref. 21(*f*) for the entire molecule, except for the nickel(II) atom and the atoms of the propylene bridge; (3) all hydrogen atoms were placed in calculated positions, with displacement parameters 10% larger than those of the atom they were attached to. Methyl groups were refined as rigid rotors with idealized distances and angles; rotation of this rigid rotor about the C–C bond was allowed. Atomic scattering factors were from ref. 21(*g*).

Low-temperature structures of complexes 5, 9 and 19. For complexes **5**, **10** and **19** the entire data sets were obtained over 6 (**5** and **10**) or 10 h (**19**) by using a Siemens SMART-CCD X-ray system. Data were processed by using Siemens SMART system software and the Siemens SAINT program for integration of data frames. Corrections for Lorentz-polarization effects were applied. Data were corrected for absorption (SADABS [21h]). The structures were solved by direct methods.[21a] The coordinates and anisotropic displacement parameters for all non-hydrogen atoms were refined by full-matrix least-squares methods.[21a] Hydrogen atoms were included in the structural model at calculated positions. The carbon atoms bridging the two halves of the ligand in **19** were disordered; the site occupation factors for these atoms were fixed at 50% in the final cycles of refinement. For these bridge atoms of **19** a constraint was applied to the bond between C(20A) and C(22A) to fix its length at a reasonable value.

CCDC reference number 186/717.

Acknowledgements

We gratefully acknowledge Mette Maagaard and Niels J. Poulsen, Aarhus University (Aa. U.), for their participation in the structure determination of complex **5**, Svend U. Hansen, Karsten N. Koch and Lene Mogensen (Aa. U.) for their participation in the structure determination of **14**, Carsten Buch and Birthe Haack, Odense University (O. U.), for technical assistance with collection of NMR spectra, Inge Pedersen and Ole T. Sørensen (O. U.) for the mass spectra, the Danish Natural Science Research Council and the Carlsberg Foundation for the Huber diffractometer at Aa. U., and the National Institutes of Health (U. S. Grant Number 1510RR10547-01) for the Siemens SMART-CCD diffractometer at Colorado State University.

References

1 (*a*) I. Y. Kvitko, L. V. Alam, N. I. Rtishchev, A. V. Eltsov, L. N. Kuriovskaya and N. B. Chebotareva, *J. Gen. Chem. USSR*, 1982, 2048; (*b*) A. la Cour, M. Findeisen, K. Hansen, R. Hazell, L. Hennig, C. E. Olsen, L. Petersen and O. Simonsen, *J. Chem. Soc.*, *Dalton Trans.*, 1997, 2045; (*c*) H. Toftlund, A. L. Nivorozhkin, A. la Cour, B. Adhikhari, K. S. Murray, G. D. Fallon and L. E. Nivorozhkin, *Inorg. Chim. Acta*, 1995, **228**, 237; (*d*) V. P. Garnovskii, V. P. Kurbatov, B. A. Porai-Koshits, O. A. Osipov, I. Y. Kvitko, L. S. Minkina, E. M. Sofina and A. F. Soloshko-Doroshenko, *J. Gen. Chem. USSR*, 1970, 2326; (*e*) A. la Cour, M. Findeisen, A. Hazell, L. Hennig, G. Zdobinsky and O. Simonsen, unpublished work; (*f*) A. la Cour, B. Adhikhari, H. Toftlund and A. Hazell, *Inorg. Chim. Acta*, 1992, **202**, 145; (*g*) A. D. Garnovskii, A. L. Nivorozhkin and V. I. Minkin, *Coord. Chem. Rev.*, 1993, **126**, 1.

2 (*a*) S. Yamada, *Coord. Chem. Rev.*, 1966, **1**, 415; (*b*) R. Knorr and A. Weiss, *Chem. Ber.*, 1981, **114**, 2104; (*c*) J. M. Fernandez-G., M. J. Rosales-Hoz, M. F. Rubio-Arroyo, R. Salcedo, F. Toscano and A. Vela, *Inorg. Chem.*, 1987, **26**, 349.

3 (*a*) D. H. Gerlach and R. H. Holm, *J. Am. Chem. Soc.*, 1969, **91**, 3457; (*b*) W. S. Sheldrick, R. Knorr and H. Polzer, *Acta Crystallogr.*, *Sect. B*, 1979, **35**, 739; (*c*) M. Schumann and H. Elias, *Inorg. Chem.*, 1985, **24**, 3187; (*d*) E. Uhlemann, G. Hinsche, H. Braunschweig and M. Weissenfels, *Z. Anorg. Allg. Chem.*, 1970, **377**, 321; (*e*) I. Bertini, L. Sacconi and G. P. Speroni, *Inorg. Chem.*, 1972, **11**, 1323.

4 (*a*) V. A. Kogan, N. N. Kharabaev, O. A. Osipov and S. G. Kochin, *J. Struct. Chem.*, 1981, **22**, 96; (*b*) O. P. Anderson, J. Becher, H. Frydendahl, L. F. Taylor and H. Toftlund, *J. Chem. Soc.*, *Chem. Commun.*, 1986, 699; (*c*) C. T. Pedersen, *Sulfur Rep.*, 1980, **1**, 1; (*d*) C. T. Pedersen, *Phosphorus Sulfur Silicon*, *Relat. Elem.*, 1991, **58**, 17; (*e*) J. Roncali, L. Rasmussen, C. Thobie-Gautier, P. Frère, H. Brisset, M. Sallé, J. Becher, O. Simonsen, T. K. Hansen, A. Benahmed-Gasmi, J. Orduna, J. Garin, M. Jubault and A. Gorgues, *Adv. Mater.*, 1994, **6**, 841.

5 E. Frason, C. Panattoni and L. Sacconi, *J. Phys. Chem.*, 1959, **63**, 1908; S. C. Chang, D. Y. Park and N. C. Li, *Inorg. Chem.*, 1968, **7**, 2144; E. E. Castellano, O. J. R. Hodder, C. K. Prout and P. J. Sadler, *J. Chem. Soc. A*, 1971, 2620; L. L. Merritt, jun., C. Guaret and A. E. Lessor, jun., *Acta Crystallogr.*, 1956, **9**, 253.

6 (*a*) W. C. Hoyt and G. W. Everett, jun., *Inorg. Chem.*, 1969, **8**, 2030; (*b*) G. M. Mockler, G. W. Chaffey, E. Sinn and H. Wong, *Inorg. Chem.*, 1972, **11**, 1308; (*c*) M. A. A. F. de C. T. Carrondo, B. de Castro, A. M. Coelho, D. Doningues, C. Freire and J. Morais, *Inorg. Chim. Acta*, 1993, **205**, 157; (*d*) M. Green and P. A. Tasker, *J. Chem. Soc. A*, 1970, 2531; (*e*) M. Green and P. A. Tasker, *Inorg. Chim. Acta*, 1971, **5**, 65; (*f*) B. M. Higson and E. D. McKenzie, *J. Chem. Soc. A*, 1971, 269.

7 (*a*) L. Beyer, M. Pulst, H. R. Paul and E. Hoyer, *J. Prakt. Chem.*, 1975, **317**, 265; (*b*) H. S. Jensen, V. McKee and C. J. McKenzie, personal communication; (*c*) T. Yamamura, M. Tadokoro and R. Kuroda, *Chem. Lett.*, 1989, 1246; (*d*) P. R. Blum, R. M. C. Wei and S. C. Cummings, *Inorg. Chem.*, 1974, **13**, 450; (*e*) D. Attanasio, G. Dessy, V. Fares and G. Pennesi, *Mol. Phys.*, 1980, **40**, 269.

8 (*a*) H. R. Engeseth, D. R. McMillin and E. L. Ulrich, *Inorg. Chim. Acta*, 1982, **67**, 145; (*b*) M. J. O'Connor, R. E. Ernst and R. H. Holm, *J. Am. Chem. Soc.*, 1968, **90**, 4561; (*c*) M. J. O'Connor and R. H. Holm, *Prog. Inorg. Chem.*, 1971, **14**, 241; (*d*) H. Frydendahl, H. Toftlund, J. Becher, J. C. Dutton, K. S. Murray, L. F. Taylor, O. P. Anderson and E. R. T. Tiekink, *Inorg. Chem.*, 1995, **34**, 4467.

9 (*a*) A. la Cour, M. Findeisen, R. Hazell, L. Hennig, C. E. Olsen and O. Simonsen, *J. Chem. Soc.*, *Dalton Trans.*, 1996, 3437 and refs. therein; (*b*) L. Hennig, R. Kirmse, O. Hammerich, S. Larsen, H. Frydendahl, H. Toftlund and J. Becher, *Inorg. Chim. Acta*, 1995, **234**, 67.

10 A. N. Nivorozhkin, H. Toftlund, P. L. Jørgensen and L. E. Nivorozhkin, *J. Chem. Soc.*, *Dalton Trans.*, 1996, 1215.

11 A. la Cour, Ph. D. Thesis, Odense University, Odense, 1996.

12 (*a*) O. P. Anderson, A. la Cour, M. Findeisen, L. Hennig, L. F. Taylor, O. Simonsen and H. Toftlund, *J. Chem. Soc.*, *Dalton Trans.*, 1997, 111; (*b*) C. P. Brock and J. D. Dunitz, *Chem. Mater.*, 1994, **6**, 1118; (*c*) K. Bernardo, S. Leppard, A. Robert, G. Commenges, F. Dahan and B. Meunier, *Inorg. Chem.*, 1996, **35**, 387.

13 (*a*) F. Akhtar and M. G. B. Drew, *Acta Crystallogr.*, *Sect. B*, 1982, **38**, 1149; (*b*) M. G. B. Drew, R. N. Prasad and R. P. Sharma, *Acta Crystallogr.*, *Sect. C*, 1985, **41**, 1755; (*c*) F. Akhtar, *Acta Crystallogr.*, *Sect. B*, 1981, **37**, 84; (*d*) N. A. Bailey, E. D. McKenzie and J. M. Worthington, *J. Chem. Soc.*, *Dalton Trans.*, 1974, 1363; (*e*) E. M. Martin, R. D. Bereman and P. Singh, *Inorg. Chem.*, 1991, **30**, 957; (*f*) A. L. Nivorozhkin, L. E. Konstantinovsky, L. E. Nivorochkin, V. I. Minkin, T. G. Takhirov, O. A. Diachenko and D. B. Tagiev, *Izv. Akad. Nauk SSSR*, *Ser. Khim.*, 1990, 327 (in Russian); (*g*) A. la Cour, M. Findeisen, A. Hazell, R. Hazell and G. Zdobinsky, *J. Chem. Soc.*, *Dalton Trans.*, 1997, 121.

14 (*a*) J. H. Weber, *Inorg. Chem.*, 1967, **6**, 258; (*b*) E. M. Martin, R. D. Bereman and J. Dorfman, *Inorg. Chim. Acta*, 1990, **176**, 247; (*c*) E. M. Martin and R. D. Bereman, *Inorg. Chim. Acta*, 1991, **188**, 221.

15 (*a*) M. Gerloch, *Coord. Chem. Rev.*, 1990, **99**, 117; (*b*) A. Ceulemans, M. Dendooven and L. G. Vanquickenborne, *Inorg. Chem.*, 1985, **24**, 1159.

16 A. B. P. Lever, *Inorganic Electronic Spectroscopy*, 2nd edn., Elsevier, Amsterdam, 1984, pp. 218–223.

17 (*a*) T. Yamamura, M. Tadokoro, M. Hamaguchi and R. Kuroda,

Chem. Lett., 1989, 1481; (*b*) R. D. Bereman, J. R. Dorfman, J. Bordner, D. P. Rillema, P. McCarthy and G. D. Shields, *J. Bioinorg. Chem.*, 1982, **16**, 47; (*c*) M. Culotti, L. Casella, A. Pintar, E. Suardi, P. Zanello and S. Mangani, *J. Chem. Soc.*, *Dalton Trans.*, 1989, 1979.
18 F. Woldby, *Studies of Optical Activity*, Polyteknisk Forlag, Copenhagen, 1973, pp. 134, 180 (in Danish); F. H. Dickey, W. Ficket and H. J. Lucas, *J. Am. Chem. Soc.*, 1952, **74**, 944.
19 C. Harries and T. Haga, *Ber. Dtsch. Chem. Ges.*, 1898, **31**, 550; 1899, **32**, 1191.
20 J. Becher, K. Pluta, N. Krake, K. Brøndum, N. J. Christensen and M. V. Vinader, *Synthesis*, 1985, 530; J. Becher, P. L. Jørgensen, H. Frydendahl and B. Fält Hansen, *Synthesis*, 1991, 609.
21 (*a*) G. M. Sheldrick, SHELXTL, version 5, Siemens Analytical X-Ray Division, Madison, WI, 1994; (*b*) M. S. Lehmann and F. K. Larsen, *Acta Crystallogr.*, *Sect. A*, 1974, **30**, 580; (*c*) G. M. Sheldrick, SHELXS 86, Program for the Solution of Crystal Structures, University of Göttingen, 1986; (*d*) W. T. Busing, K. O. Martin and H. A. Levy, ORFLS, Report ORNL-TM-306, Oak Ridge National Laboratory, Oak Ridge, TN, 1962; (*e*) G. S. Pawley, in *Advances in Structure Research by Diffraction Methods*, eds. W. Hoppe and R. Mason, Pergamon, Oxford, 1971, vol. 4, pp. 1–64; (*f*) V. Schomaker and K. N. Trueblood, *Acta Crystallogr.*, *Sect. B*, 1968, **24**, 63; (*g*) *International Tables for X-Ray Crystallography*, Kynoch Press, Birmingham, 1974, vol. 4, pp. 72–98; (*h*) SADABS, a program for Siemens area detector absorption corrections, G. M. Sheldrick, unpublished work.

Received 12*th May* 1997; *Paper* 7/03258G